

TeV GAMMA-RAY OBSERVATIONS OF THE GALACTIC CENTER

K. KOSACK,¹ H. M. BADRAN,² I. H. BOND,³ P. J. BOYLE,⁴ S. M. BRADBURY,³ J. H. BUCKLEY,¹ D. A. CARTER-LEWIS,⁵ O. ÇELİK,⁶ V. CONNAUGHTON,⁷ W. CUI,⁸ M. DANIEL,⁵ M. D’VALI,³ I. DE LA CALLE PEREZ,³ C. DUKE,⁹ A. FALCONE,⁸ D. J. FEGAN,¹⁰ S. J. FEGAN,¹¹ J. P. FINLEY,⁸ L. F. FORTSON,^{12,13} J. A. GAIDOS,⁸ S. GAMMELL,¹⁰ K. GIBBS,¹¹ G. H. GILLANDERS,¹⁴ J. GRUBE,³ K. GUTIERREZ,¹ J. HALL,¹⁵ T. A. HALL,¹⁶ D. HANNA,¹⁷ A. M. HILLAS,³ J. HOLDER,³ D. HORAN,¹¹ A. JARVIS,⁶ M. JORDAN,¹ G. E. KENNY,¹⁴ M. KERTZMAN,¹⁸ D. KIEDA,¹⁵ J. KILDEA,¹⁷ J. KNAPP,³ H. KRAWCZYNSKI,¹ F. KRENNRICH,⁵ M. J. LANG,¹⁴ S. LE BOHEC,⁵ E. LINTON,⁴ J. LLOYD-EVANS,³ A. MILOVANOVIC,³ J. MCENERY,¹⁹ P. MORIARTY,²⁰ D. MULLER,⁴ T. NAGAI,¹⁵ S. NOLAN,⁸ R. A. ONG,⁶ R. PALLASSINI,³ D. PETRY,¹⁹ B. POWER-MOONEY,¹⁰ J. QUINN,¹⁰ M. QUINN,²⁰ K. RAGAN,¹⁷ P. REBILLOT,¹ P. T. REYNOLDS,²¹ H. J. ROSE,³ M. SCHROEDTER,¹¹ G. H. SEMBROSKI,⁸ S. P. SWORDY,⁴ A. SYSON,³ V. V. VASSILIEV,⁶ S. P. WAKELY,⁴ G. WALKER,¹⁵ T. C. WEEKES,¹¹ AND J. ZWEERINK⁶

Received 2004 March 17; accepted 2004 May 11; published 2004 May 18

ABSTRACT

We report a possible detection of TeV gamma rays from the Galactic center by the Whipple 10 m gamma-ray telescope. Twenty-six hours of data were taken over an extended period from 1995 through 2003 resulting in a total significance of 3.7σ . The measured excess corresponds to an integral flux of $1.6 \times 10^{-8} \pm 0.5 \times 10^{-8}$ (stat) $\pm 0.3 \times 10^{-8}$ (sys) photons $\text{m}^{-2} \text{s}^{-1}$ above an energy of 2.8 TeV, roughly 40% of the flux from the Crab Nebula at this energy. The 95% confidence region has an angular extent of about $15'$ and includes the position of Sgr A*. The detection is consistent with a point source and shows no evidence of variability.

Subject headings: dark matter — Galaxy: center — Galaxy: nucleus — gamma rays: observations

1. INTRODUCTION

The central region of our Galaxy is now thought to contain a supermassive black hole of $2.6 \times 10^6 M_{\odot}$ (Ghez et al. 2002; Schödel et al. 2002) coincident with the unresolved radio source

¹ Department of Physics, Washington University, Campus Box 1105, St. Louis, MO 63130; kosack@hbar.wustl.edu, buckley@wuphys.wustl.edu.

² Department of Physics, Tanta University, Tanta Egleish Street, Tanta, Egypt.
³ Department of Physics, University of Leeds, Leeds, LS2 9JT Yorkshire, England, UK.

⁴ Enrico Fermi Institute, University of Chicago, 5640 South Ellis Avenue, Chicago, IL 60637.

⁵ Department of Physics and Astronomy, Iowa State University, 203 Van Allen Hall, Ames, IA 50011-3160.

⁶ Department of Physics, University of California at Los Angeles, Box 951547, Knudsen Hall, Los Angeles, CA 90095-1562.

⁷ Gamma-Ray Astrophysics Group National Space Science and Technology Center, Huntsville, AL.

⁸ Department of Physics, Purdue University, 525 Northwestern Avenue, West Lafayette, IN 47907.

⁹ Department of Physics, Grinnell College, P.O. Box 805, Grinnell, IA 50112-1690.

¹⁰ Department of Experimental Physics, National University of Ireland, Belfast, Dublin 4, Ireland.

¹¹ Fred Lawrence Whipple Observatory, Harvard-Smithsonian Center for Astrophysics, P.O. Box 97, Amado, AZ 85645-0097.

¹² Department of Astronomy and Astrophysics, University of Chicago, 5640 South Ellis Avenue, Chicago, IL 60637.

¹³ Department of Astronomy, Adler Planetarium and Astronomy Museum, 1300 South Lake Shore Drive, Chicago, IL 60605.

¹⁴ Department of Physics, National University of Ireland, Galway, Ireland.

¹⁵ High Energy Astrophysics Institute, University of Utah, 115 S 1400 E, Salt Lake City, UT 84112.

¹⁶ Department of Physics and Astronomy, University of Arkansas at Little Rock, 2801 South University Avenue, Little Rock, AR 72204-1099.

¹⁷ Department of Physics, McGill University, Ernest Rutherford Physics Building, 3600 University Street, Montreal, QC H3A 2T8, Canada.

¹⁸ Department of Physics and Astronomy, DePauw University, 101 East Seminary Street, Greencastle, IN 46135-0037.

¹⁹ University of Maryland, Baltimore County, and NASA Goddard Space Flight Center, Greenbelt, MD 20771.

²⁰ School of Science, Galway-Mayo Institute of Technology, Galway, Ireland.

²¹ Department of Applied Physics and Instrumentation, Cork Institute of Technology, Cork, Ireland.

Sgr A* (Balick & Brown 1974). *Chandra* observations reveal X-ray emission from an unresolved point source as well as an extended structure ($\sim 1''5$), both of which appear to be physically associated with Sgr A* (e.g., Baganoff et al. 2003). The recent discovery of hour-scale X-ray (Baganoff et al. 2001) and rapid IR flaring (Ghez et al. 2004) points to an active nucleus, albeit with very low bolometric luminosity compared with the luminosity inferred from the Bondi accretion rate or with that which is typical of more powerful active galactic nuclei. More recently, the *International Gamma-Ray Astrophysics Laboratory* has detected time-variable 20–100 keV emission from within $0'9$ of Sgr A* (Bélanger et al. 2004). Polarization measurements show the signature of synchrotron radiation in a Keplerian accretion disk (Liu & Melia 2002). Taken together, these multiwavelength data are not easily described by a one-component model, and the current theoretical framework combines thermal emission from a radiatively inefficient Keplerian accretion flow with synchrotron inverse Compton emission produced by electrons accelerated either in the disk or further out in a hypothetical jetlike outflow (e.g., Liu & Melia 2002; Yuan et al. 2002, 2003). From the present measurements, the maximum energy of the nonthermal electron distribution in the jet models is ambiguous, and theories alternately explain the high-energy emission as inverse Compton or the high-energy extension of the synchrotron spectrum; gamma-ray measurements may eventually break this degeneracy.

The EGRET experiment detected a strong unidentified source of GeV gamma rays marginally consistent with the position of the Galactic center (GC; Hartman et al. 1999). Both the Whipple and the Cangaroo groups have presented preliminary evidence for TeV emission at the position of Sgr A* as well (Buckley et al. 1997; Tsuchiya et al. 2003; Kosack et al. 2003). Hooper & Dingus (2002) reanalyzed the higher energy gamma-ray data from EGRET and found that the most likely position of the EGRET source may be offset from Sgr A*. However, systematic uncertainties in the gamma-ray background models and limited angular resolution make the analysis

of the source in the GC region difficult. Observations of the GC are complicated since Sgr A* is surrounded by a dense cluster of stars and stellar remnants (including low-mass X-ray binaries and black hole candidates), molecular clouds, and a large structure that may be the remnant of a powerful supernova remnant, Sgr A East (Fatuzzo & Melia 2003). Source confusion is particularly difficult for high-energy gamma-ray observations given the limited angular resolution of present experiments.

High-energy gamma-ray observations of the GC are also the subject of particular theoretical interest given the possibility of detecting halo dark matter in our galaxy (e.g., Bergström et al. 1998). Sgr A*, at the dynamical center of our Galaxy, may well be surrounded by a cusp or spike in the dark matter halo distribution (e.g., Dubinski & Carlberg 1991; Navarro et al. 1996; Gondolo & Silk 1999; Merritt 2004). Annihilation of these hypothetical weakly interacting massive particles could also contribute to the luminosity in the vicinity of Sgr A* in the radio through a gamma-ray wave band. Annihilation of dark matter would be enhanced by a factor proportional to the density squared and might result in an observable gamma-ray line (from direct annihilation to gamma rays) as well as continuum emission (from secondary products of annihilation to quarks and fermions; e.g., Silk & Bloemen 1987; Bergström 1989; Giudice & Griest 1989; Jungman & Kamionkowski 1995). The presence of a massive black hole could further steepen the density profile of the dark matter halo, producing very high radio and gamma-ray fluxes that exceed the observational upper bounds (Gondolo & Silk 1999). The details of the halo model on scales less than 100 pc and the formation history of the central black hole are critical to predicting the gamma-ray flux but are, unfortunately, still poorly understood.

Given the limited angular resolution of GeV and TeV instruments, a number of different sources could contribute to a signal near the GC. The key to distinguishing between all of the possible emission scenarios is to measure the position, angular extent, variability, and spectrum of the gamma-ray signal. Here we present first results from an analysis of Whipple telescope data. In § 2, we describe the observational method and data analysis procedure used to observe the GC at TeV energies. In § 3, we discuss a possible weak detection and consider its impact on various gamma-ray production scenarios in § 4.

2. DATA ANALYSIS

Imaging atmospheric Cerenkov telescopes, such as the Whipple Gamma-Ray Observatory, detect high-energy photons by imaging the flashes of Cerenkov light emitted by secondary particles in gamma-ray-induced air showers. The Whipple Telescope's 10 m mirror focuses the faint UV/blue Cerenkov flashes into a camera consisting of photomultiplier tube pixels. Off-line software analysis characterizes each candidate shower image, separates the signal (gamma-ray-like) from background (cosmic-ray-like) events, and determines the point of origin and energy of each gamma ray. Whipple gamma-ray data are traditionally taken as a series of 28 minute exposures, each of which is followed by an off-source run that is offset 30 minutes in right ascension for background subtraction. In the case of Sgr A*, data were taken off-source before the on-source observations because of a bright star field in the region 30 minutes past the GC's position.

Using the techniques based on the moment fitting procedure outlined in Lessard et al. (2001), we parameterize the roughly elliptical gamma-ray images by calculating moments of the

light distribution in the camera. Geometric selection criteria based on these parameters allow for the rejection of background (e.g., cosmic-ray-induced showers). The first moments give the centroid of the image, and the second moments give the *width* (minor axis) and *length* (major axis) and orientation angle of the image. The elongation of the ellipse is used to determine the point of origin of the shower. Of the two possible points of origin for each image, the asymmetry (or skew) of the shower is used to select the correct one whenever possible.

The GC ($\alpha = 17^{\text{h}}45^{\text{m}}40^{\text{s}}$, $\delta = -29^{\circ}00'28''$; J2000.0) transits at a very large zenith angle (LZA; 61°) as seen from the Whipple Observatory (N31:07 latitude), which significantly alters the shower geometry and threshold energy. To properly account for the effects of LZA observations, we developed a new set of gamma-ray selection criteria that scale with zenith angle and energy according to a semiempirical form derived from simulations and optimization of LZA Crab Nebula data. The Crab Nebula was used for optimization and calibration because it is a bright, steady gamma-ray source with a known spectrum.

Furthermore, the brightness of the Galactic plane near the GC results in an increase in energy threshold and, if not compensated for, a systematic bias in the observed excess. Pedestal events, containing no image, are injected at random intervals throughout the run for calibration of Poisson fluctuations in the night-sky background. Both on and off-source data are analyzed in the same manner, and Gaussian deviates are added to the pixel signals to bring the background noise up to the same level in both runs. After this procedure, only pixels with signals well above the noise level are included in further image processing. This Gaussian padding combined with a high software trigger threshold largely removes systematic biases arising from brightness differences but increases the energy threshold.

To determine the pointing error in the telescope, we look at the pedestal variation for each camera tube. The presence of visible light from a star or other source in the field of view adds to the pedestal variance in the corresponding pixel. Using this effect, we can generate a crude optical image of the sky by accumulating the pedestal variations of each pixel in a two-dimensional histogram. Using this technique, an optical sky-brightness map is generated for each observation. By comparing the bright spots in the Sgr A* image (or special runs where the telescope is pointed at a nearby pointing-check star) we can obtain an absolute measure of the pointing error. In addition, we cross-correlate each pair of maps to determine the relative pointing offset between them. We keep only runs that have the correct star field and have a relative pointing offset that is less than the diameter of 1 pixel. We find residual pointing errors of $\pm 0.1^{\circ}$ at LZA. These errors are attributed in part to the fact that observations have been made near the balance point of the telescope and near the horizontal position where flexure of the optical support structure is maximal.

To correct for changes in the overall light sensitivity (throughput) of the camera between epochs, we look at muon events in data taken at each epoch. Muons, which show up as bright arcs of Cerenkov light in the camera, are useful for calibration because the light per unit arc length from a muon event is nearly constant, regardless of the impact parameter and angle of the trajectory. A measure of the throughput of the telescope can be found by comparing the signal/arc length distribution to a set of simulated muon events. These were generated as secondaries to proton and helium showers using the Grinnell/ISU simulation package. The relative throughput was found to have changed by a factor of 2.22 between 1995

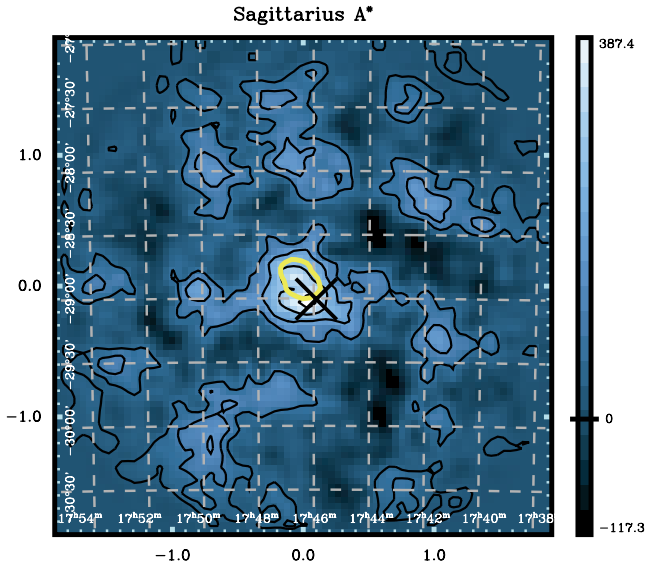


FIG. 1.—Gamma-ray image of the region around Sgr A*. The image is of excess counts with overlaid significance contours (1σ per contour). The axes are labeled in degrees from the assumed camera center. The true center position of the camera, which is not exactly at (0, 0) because of flexing of the telescope at low elevation, is marked with a cross. The dashed lines are the R.A. and decl. contours at this position. Also shown (as a light contour) is the 99% confidence region for the EGRET observations (Hooper & Dingus 2002).

and 2001. We scale the software trigger threshold and energy estimator by this factor so the trigger cuts are consistent across observations. This method also serves to calibrate the simulations used to determine the peak energy at LZA.

Our data on Sgr A* span several epochs during which the Whipple camera was upgraded twice. During the 1995–1996 observing seasons, the camera consisted of 109 pixels (each with $0^\circ.26$ diameter); it was upgraded at the end of 1996 to 151 pixels and again in 1999 to 379 smaller diameter ($0^\circ.12$) pixels. In order to combine all of these data, we developed a method to scale our gamma-ray selection criteria with pixel size.

As one observes at increasing zenith angles, the distance to the core of the air shower increases, and thus the angular size of the shower and parallactic displacement of the image centroid are reduced. To derive the scaling laws, we first assume that the width and length of gamma-ray air shower images are approximately proportional to $\cos^\alpha \theta$, where θ is the zenith angle and α is a constant. In addition, air shower simulations show that length and width scale as the logarithm of the energy, which is proportional to the total camera signal (S) of the event. Combining these results, and removing the effects of the finite pixel size of the camera (σ_{pix}) and the point-spread function of the telescope (σ_{psf}), the measured length (L), width (W), and the distance to the image centroid (D) can be converted to scaled values L' , W' , and D' by the following equations: $L' \approx [(L^2 - \sigma_{\text{pix}}^2 - \sigma_{\text{psf}}^2) / \cos^{1.5} \theta]^{1/2} - 0.023 (\ln S - 8)$, $W' \approx [(W^2 - \sigma_{\text{pix}}^2 - \sigma_{\text{psf}}^2) / \cos^{1.2} \theta]^{1/2} - 0.020 (\ln S - 8)$, and $D' \approx D / \cos \theta$.

The constant factors and cosine powers were derived from simulations. Data selection criteria $0^\circ.125 < L' < 0^\circ.3$, $0^\circ.05 < W' < 0^\circ.135$, and $0^\circ.28 < D' < 2^\circ.2$ are applied to select candidate gamma-ray events. Cuts based on these intrinsic parameters were verified to be independent of zenith angle and camera design by application of this method to independent Crab Nebula data taken over the period 1994–2003.

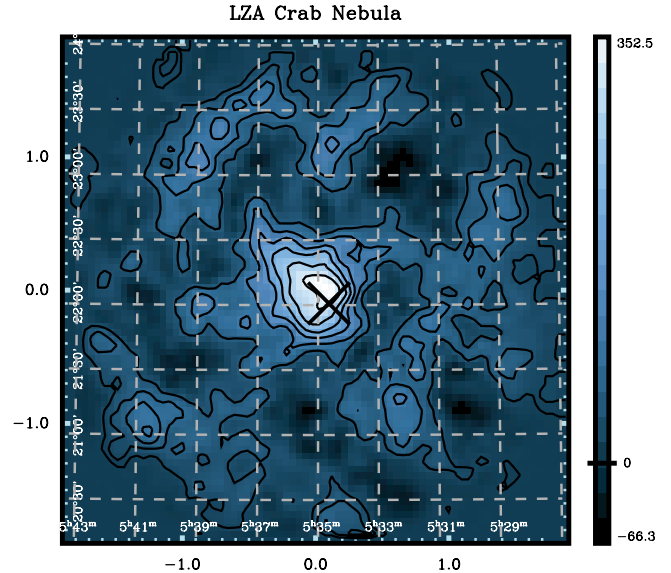


FIG. 2.—Gamma-ray image of the Crab Nebula taken at LZA ($\approx 62^\circ$) using the same analysis procedure used for Sgr A*. The offset and pointing variations can be seen in the resulting image.

3. RESULTS

We have combined all observations of Sgr A* from 1995 through 2003 resulting in 26 hr of on-source exposure at an average zenith angle of 61° . To determine the pointing offset, observations were taken centered on a nearby bright star (Sgr γ_2) which is at the same elevation as Sgr A*. Using the sky-brightness map technique outlined earlier, we determined that the telescope had a pointing offset of $0^\circ.14$. Figure 1 shows the resulting two-dimensional map of gamma-ray excess with overlaid significance contours. The true center of the camera, correcting for the offset, is plotted as a cross in the image. This image shows a 4.2σ excess at the corrected center position. To check the robustness of this result, we reran the analysis 10 times to account for variations due to the Gaussian padding. We find that the average significance at the corrected center position is $(3.7 \pm 0.13)\sigma$, somewhat below the initial result. For reference, in Figure 2 we show the results of the same analysis procedure applied to 10 hr of observations of the Crab Nebula at a similar zenith angle range. Note that the significance of 6.1σ of the Crab detection at the offset position is substantially higher than the result of 3.8σ obtained applying the standard small zenith angle analysis procedure to these LZA data. Also, the similar angular extent in the two results indicates consistency with a point source within a 95% confidence region of radius $\approx 15'$.

To determine the peak energy of the detected flux from Sgr A*, we simulated gamma rays with a Crab Nebula spectrum (with integral spectral index $\gamma = 1.58$; Mohanty et al. 1998) and a zenith angle of 61° and analyzed the resulting data with a detector simulation and our analysis software. We determined the peak detected energy to be ≈ 2.8 TeV, with a 20% systematic error in this energy threshold. We then analyzed a set of contemporaneous LZA Crab Nebula data runs to find the Crab count rate and compared this to the corresponding rate for Sgr A*. The integral flux for Sgr A*, normalized to the Crab flux, is then $F_{\text{Sgr A}^*}(> 2.8 \text{ TeV}) = N_{0, \text{Crab}} (2.8 \text{ TeV})^{-\gamma} / \gamma (R_{\text{Sgr A}^*} / R_{\text{Crab}})$, where $N_{0, \text{Crab}}$ is the flux normalization factor for the Crab Nebula ($3.12 \times 10^{-7} \text{ m}^{-2} \text{ s}^{-1}$), γ is the integral Crab spectral index, and $R_{\text{Sgr A}^*}$ and R_{Crab} are the

corresponding Sgr A* and Crab Nebula gamma-ray count rates. From the LZA Crab data, we find a gamma-ray rate of $R_{\text{Crab}}(> 2.8 \text{ TeV}) = 0.501 \pm 0.087$ photons minute⁻¹, and from Sgr A* we obtain an average rate of $R_{\text{Sgr A*}}(> 2.8 \text{ TeV}) = 0.205 \pm 0.057$ photons minute⁻¹. Hence, the gamma-ray flux from the GC region above 2.8 TeV is $1.6 \times 10^{-8} \pm 0.5 \times 10^{-8}$ (stat) $\pm 0.3 \times 10^{-8}$ (sys) photons m⁻² s⁻¹, or about 0.4 times that of the Crab Nebula (the flux error includes the uncertainty in the Crab Nebula measurement).

To determine the probability for steady emission, a χ^2 fit of a constant function was applied to this data and, for comparison, to a series of data taken of Mrk 421 (a source that is known to be highly variable) at a similar zenith angle range as Sgr A*. The total significance of this Mrk 421 data sample was 2.3 σ . The Sgr A* data yield a constant count rate of (0.22 ± 0.05) γ minute⁻¹ with a reduced χ^2 of 1.13 (with 54 degrees of freedom), which corresponds to a 25% probability that there is no variability. The result for Mrk 421 yields a constant count rate of (0.25 ± 0.21) γ minute⁻¹ with a reduced χ^2 of 3.03 (with 6 degrees of freedom) and a 1.2% chance of no variability.

4. DISCUSSION

The TeV excess observed near the position of the GC is unlikely to have occurred by chance and constitutes a probable, as yet unconfirmed, detection of a new TeV source. Possible systematics that could contribute to a false detection include the effects of additional noise from the relatively bright off-source region. While we have largely corrected for these effects, some systematic uncertainties remain. We have taken into account trials factors by formulating an explicit a priori hypothesis that we would only look for emission at the exact position of the GC after a pointing correction was applied. Statistical variations in the analysis method (due to the addition of simulated noise in padding) have been taken into account by repeating the analysis 10 times and taking the average significance, giving a conservative estimate of 3.7 σ for the detection significance.

The lack of significant variability in our data makes it difficult to uniquely identify the source with a compact point source such as Sgr A* but inspires some confidence in the stability of our observations at LZA. Note that the analysis procedure was designed to mitigate against changes in the count rate due to variations in the instrument. The same ISU simulation package used here was used previously to analyze LZA Whipple observations of the Crab Nebula, giving a spectrum in good agreement with that measured at small zenith angles (Krennrich et al. 1999). In

the past, our group reported a positive excess of 2.4 σ for 1995–1997 observations (Buckley et al. 1997) and 2.4 σ for 1999–2003 observations (Kosack et al. 2003) at the position of Sgr A*. The combined significance is consistent with these earlier analyses. The large error circles for both EGRET (7'2) and Whipple (15') observations make identification with a particular source difficult, but given the dearth of TeV sources, an accidental angular coincidence of a new source along the line of sight is unlikely, and it is probable that the emission comes from a nonthermal source physically near the GC.

The high level of emission ≈ 0.4 crab at a distance of roughly 4 times that of the Crab Nebula qualifies this as an unusually luminous galactic source. Previous TeV observations of relatively nearby galactic sources such as X-ray binaries and shell-type and plerionic supernovae have produced numerous upper limits, or (at best) unconfirmed detections, making the detection of such an object at 8.5 kpc even more unlikely. Mayer-Hasselwander et al. (1998) came to a similar conclusion about the GeV emission based on the high luminosity of the EGRET unidentified source and lack of significant variability. If the Sgr A East supernova shock were the source of the EGRET gamma rays, it would have been an unusually intense explosion (Khokhlov & Melia 1996), and a density of 1000 cm⁻³ and magnetic field of $B \sim 0.18$ mG (well above the canonical values) would be required (Fatuzzo & Melia 2003). While a typical galactic source such as a supernova remnant, pulsar, or stellar mass black hole is unlikely, an association with Sgr A* is still a viable possibility, and the detection of correlated variability in future gamma-ray and X-ray observations could make the identification compelling. If we associate this emission with either the supermassive black hole Sgr A* or the supernova remnant Sgr A East, the observed emission could come from self-Compton scattering by electrons with energies up to at least 2.8 TeV or from pion-decay gamma-rays from primary protons of even higher energy (kinematics require their energy to be at least several times the maximum gamma-ray energy). The lack of significant variability and the consistency with the GC position allow more exotic possibilities such as the annihilation of very high mass (> 2 TeV) dark matter particles at the GC.

We would like to acknowledge Fulvio Melia, Paolo Gondolo, Jonathan Katz, and Ramanath Cowsik for useful discussions. The VERITAS Collaboration is supported by the US Department of Energy, NSF, the Smithsonian Institution, PPARC (UK), NSERC (Canada), and Enterprise-Ireland.

REFERENCES

- Baganoff, F. K., et al. 2001, *Nature*, 413, 25
 ———. 2003, *ApJ*, 591, 891
 Balick, B., & Brown, R. L. 1974, *ApJ*, 194, 265
 Bélanger, G., et al. 2004, *ApJ*, 601, L163
 Bergström, L. 1989, in *Particle Astrophysics: Forefront Experimental Issues*, ed. E. B. Norman (Singapore: World Scientific), 255
 Bergström, L., Ullio, P., & Buckley, J. H. 1998, *Astropart. Phys.*, 9, 137
 Buckley, J. H., et al. 1997, *Proc. 25th Int. Cosmic Ray Conf. (Durban)*, 237
 Dubinski, J., & Carlberg, R. G. 1991, *ApJ*, 378, 496
 Fatuzzo, M., & Melia, F. 2003, *ApJ*, 596, 1035
 Ghez, A. M., et al. 2002, *BAAS*, 34, 1219
 ———. 2004, *ApJ*, 601, L159
 Giudice, G. F., & Griest, K. 1989, *Phys. Rev. D*, 40, 2549
 Gondolo, P., & Silk, J. 1999, *Phys. Rev. Lett.*, 83, 1719
 Hartman, R. C., et al. 1999, *ApJS*, 123, 79
 Hooper, D., & Dingus, B. 2002, preprint (astro-ph/0212509)
 Jungman, G., & Kamionkowski, M. 1995, *Phys. Rev. D*, 51, 3121
 Khokhlov, A., & Melia, F. 1996, *ApJ*, 457, L61
 Kosack, K., et al. 2003, *Proc. 28th Int. Cosmic Ray Conf. (Tsukuba)*, 2513
 Krennrich, F., et al. 1999, *ApJ*, 511, 149
 Lessard, R. W., Buckley, J. H., Connaughton, V., & Le Bohec, S. 2001, *Astropart. Phys.*, 15, 1
 Liu, S., & Melia, F. 2002, *ApJ*, 566, L77
 Mayer-Hasselwander, H. A., et al. 1998, *A&A*, 335, 161
 Merritt, D. 2004, *Phys. Rev. Lett.*, submitted (astro-ph/0311594)
 Mohanty, G., et al. 1998, *Astropart. Phys.*, 9, 15
 Navarro, J. F., Frenk, C. S., & White, S. D. M. 1996, *ApJ*, 462, 563
 Schödel, R., et al. 2002, *Nature*, 419, 694
 Silk, J., & Bloemen, H. 1987, *ApJ*, 313, L47
 Tsuchiya, K., et al. 2003, *Proc. 28th Int. Cosmic Ray Conf. (Tsukuba)*, 2517
 Yuan, F., Markoff, S., & Falcke, H. 2002, *A&A*, 383, 854
 Yuan, F., Quataert, E., & Narayan, R. 2003, *ApJ*, 598, 301